

1 **Title:** *Evolution of the genetic architecture of local adaptations under genetic rescue is*
2 *determined by mutational load and polygenicity*

3

4 **Running title:** *Local adaptations under genetic rescue*

5

6 **Authors:** Yulin Zhang^{1,2,*}, Aaron J. Stern^{2,*,+}, Rasmus Nielsen^{3,4,5+}

7

8 ¹School of Life Sciences, Sun Yat-sen University, Guangzhou, Guangdong, P.R.China

9 ²Graduate Group in Computational Biology, UC Berkeley, Berkeley, CA 94707, USA.

10 ³Department of Integrative Biology, UC Berkeley, Berkeley, CA 94707, USA.

11 ⁴Department of Statistics, UC Berkeley, Berkeley, CA 94707, USA.

12 ⁵Natural History Museum of Denmark, University of Copenhagen, 1350 København K,
13 Denmark.

14

15 *Authors contributed equally

16 ⁺Corresponding authors: AJS: ajstern@berkeley.edu, RN: rasmus_nielsen@berkeley.edu

17

18 **Abstract:**

19 Inbred populations often suffer from heightened mutational load and decreased fitness
20 due to lower efficiency of purifying selection at small effective population size. Genetic
21 rescue (GR) is a tool that is studied and deployed with the aim of increasing fitness of such
22 inbred populations. The success of GR is known to depend on certain factors that may vary
23 between different populations, such as their demographic history and distribution of
24 dominance effects of mutations. While we understand the effects of these factors on the
25 evolution of overall ancestry in the inbred population after GR, it is less clear what the effect
26 is on local adaptations and their genetic architecture. To this end, we conduct a population
27 genetic simulation study evaluating the effect of several different factors on the efficacy of
28 GR including trait complexity (Mendelian vs. polygenic), dominance effects, and

29 demographic history. We find that the effect on local adaptations depends highly on the
30 mutational load at the time of GR, which is shaped dynamically by interactions between
31 demographic history and dominance effects of deleterious variation. While local adaptations
32 are generally restored post-GR in the long run, in the short term they are often compromised
33 in the process of purging deleterious variation. We also show that while local adaptations are
34 almost always fully restored, the degree to which ancestral genetic variation comprising the
35 trait is replaced by donor variation can vary drastically, and is especially high for complex
36 traits. Our results provide considerations for practical GR and its effects on trait evolution.

37

38 **Keywords:** Genetic rescue; conservation genetics; local adaptations; mutational load;
39 dominance; demographic history; polygenic traits

40

41 **1. Introduction**

42 Genetic rescue (GR) is a strategy used in conservation biology to increase fitness of an
43 endangered inbred (recipient) population by introducing genetic variation from another
44 (donor) population. GR is accomplished by assisted migration of individuals from closely
45 related, healthy populations to the inbred imperiled population. This process naturally causes
46 the replacement of local genetic variation in the recipient population with that of the donor
47 population. Typically, only a small number of individuals are introduced in order to conserve
48 local genetic variation (Whiteley, Fitzpatrick, Funk & Tallmon, 2015).

49 The strategy has now been practiced on many highly inbred populations from different
50 taxa, including the Florida panther (Johnson et al., 2010), robins (Heber et al., 2012), guppies
51 (Fitzpatrick et al., 2016), wood rats (Smyser et al., 2013), and adders (Madsen et al., 1999). In
52 several cases, GR efficiently increased the absolute fitness of the inbred population and
53 reduced inbreeding depression (Frankham, 2015). A famous example is the introduction of
54 mountain lions from Texas of the sub-species *P. c. stanleyana* to the Florida *P. c. coryi*
55 population, for which the number of *P. c. coryi* increased three-fold after only five years, with
56 increased survival rates and a doubling of the heterozygosity (Johnson et al., 2010). A meta-

57 analysis provided evidence that the beneficial effect of GR can persist through the F3
58 generation (Frankham, 2016). These empirical tests suggest that GR is a powerful
59 conservation tool for increasing fitness in endangered inbred populations.

60 However, despite its promise, there is skepticism and caution towards the application of
61 GR due to concerns about outbreeding depression and genetic homogenization (Bell, *et al.*
62 2019). In the case of the Florida panther, an estimated genetic replacement of 41% has been
63 reported. In another case of the Isle Royale wolf, the immigration of one single male to Isle
64 Royale caused a genetic replacement of 56% to the local inbred population within two
65 generations (Adams et al. 2011). Hwang et al (2012) also reported a negative fitness effect
66 after practicing GR with two species that are genetically highly divergent due to outbreeding
67 depression.

68 Several different theoretical studies have been conducted to examine the expected
69 efficacy of GR (Hedrick, Hellsten & Grattapaglia, 2016; Harris, Zhang & Nielsen, 2019;
70 Tallmon et al., 2004; Frankham, et al., 2011). The dynamics of GR is complex, depending on,
71 among other factors, the amount of gene-flow, the demographic model (e.g. effective
72 population size), and the dominance coefficients of mutations. Harris et al (2019) showed that
73 with a higher amount of introgression, the relative fitness of the recipient population recovers
74 more quickly; however, this occurs at the cost of replacing an increasing proportion of the
75 recipient's ancestral genomes with those of the donor population. Demographic history of the
76 recipient and donor populations also determines the dynamics of GR. For example, small
77 effective population size (N_e) limits the efficacy of natural selection; thus, in most cases
78 admixture from a population with large N_e helps restore fitness (Harris et al., 2019). However,
79 several studies have shown that demography and dominance of deleterious mutations have
80 key interaction effects on the GR process (Harris et al., 2019; Kyriazis, Wayne & Lohmueller,
81 2019). For example, Kyriazis et al (2019) showed that fitness in populations with historically
82 low N_e can be more robust to severe bottlenecks than those with historically large N_e , as these
83 populations are less efficient at purging recessive deleterious mutations.

84 Previous studies suggest that the genetic replacement caused by GR can be controlled if

85 the amount of admixture is limited (Harris et al., 2019; Whiteley et al., 2015; Bell et al.,
86 2019). However, whether local adaptation plays a role in GR remains an open question.
87 Recently, Osmond & Coop (2019) investigated the population genetic signatures of selective
88 sweeps under evolutionary rescue, i.e. the adaptive response and recovery from reduced
89 absolute fitness due to environmental change. Also, Tomasini & Peischl (2019) investigated
90 the effect of local adaptations on evolutionary rescue. But whether GR would lead to the loss
91 of unique local adaptations, or whether local adaptations could affect the process of fitness
92 restoration by GR, remain largely unexplored.

93 Here, we explore how the addition of linked locally-adaptive variation affects the GR
94 process. Specifically, we explore the dynamics under GR of (1) a Mendelian trait, and (2) a
95 polygenic trait under stabilizing selection with a shift in the optimum. Our results illustrate
96 how the genetic architecture of adaptive traits evolve under GR, and how the dynamics of GR
97 depends on the joint effects of demographic models and genetic factors such as dominance.

98

99 **2. Materials and Methods**

100 We simulate under two demographic models from Harris, et al. (2019), as illustrated in
101 Figure 1. The simulations are conducted using SLiM (Haller & Messer, 2019). Model 1 (Fig.
102 1A) represents a population that undergoes a long-term bottleneck of 0.1 times the ancestral
103 population size ($N_e=10^4$), which last for 16,000 generations. This demographic history
104 represents a population that is inbred for a long period of time and is similarly to that
105 estimated for Neanderthals by Prufer *et al.* (2014). Neanderthals represent a good example of
106 a long-term inbred population where genomic analyses have discovered a substantial
107 accumulation of deleterious alleles (Prufer *et al.*, 2014). Model 2 (Fig. 1B) represents instead
108 a population with an extreme, short-lived bottleneck with $N_e=10$ that lasts for 20 generations,
109 which might be more representative of many currently endangered species. Prior to the time
110 of divergence, we conduct a burn-in phase of 44,000 generations. We simulate two modes of
111 adaptation: a Mendelian trait, with only one adaptive site contributing to the trait, and a
112 polygenic trait controlled by a large mutational target.

113 We simulate the Mendelian trait under two selection models: (1) a hard sweep, in which a
114 rare additive beneficial mutation occurs after the split of the population, and (2) a soft sweep
115 from a standing variant, in which an allele segregating neutrally leading up to the split is
116 picked at random, and its selection coefficient is then changed so that the allele is then
117 beneficial. Selection acts on the trait only after the split of two populations. For both models,
118 we have examined different selection coefficients, $s = 10^{-4}$, 10^{-3} , and 10^{-2} for the adaptive
119 mutation.

120 We simulate the polygenic trait under a model of stabilizing selection with Gaussian
121 fitness. To model the effects of local adaptation in the recipient population we allow the
122 phenotypic optimum in this deme to increase by some amount, immediately following the
123 divergence from the ancestral population. With V_S as the variance of the fitness function (not
124 to be confused with the variance in fitness among individuals), we simulated scenarios where
125 the inbred population's phenotypic optimum shifts by $\delta = 1, 2, 5$ immediately after the split,
126 while the phenotypic optimum remains 0 for the outbred population. We considered different
127 selection strengths by setting the variance of the fitness function to be $V_S = 3,000$ and $10,000$.
128 We assume genetic effects among loci are purely additive. Under this model, at equilibrium
129 (phenotypic mean equal to the optimum), alleles are under under-dominant selection with
130 $s = a^2/V_S$, where a is the effect of the allele, on the same scale on which the fitness
131 function is defined (Simons, *et al.* 2018). In the transient phase after a large shift in the
132 optimum, selection is approximately additive with $s = a\delta/V_S$ (Hayward & Sella, 2019). In
133 order to ensure selection coefficients of causal SNPs are roughly $s \sim 10^{-4} - 10^{-3}$, in line
134 with current estimates that SNPs ascertained for complex traits in humans have been under
135 weak selection (Simons, *et al.* 2018), we draw the effects of causal alleles (a) from a standard
136 normal distribution (i.e. mean 0 and variance 1). See Table S1 for more details.

137 In addition to the adaptive mutations described above, we also allow for accumulation of
138 deleterious mutations assumed to be (1) additive ($h=0.5$), (2) partially recessive ($h=0.1$) and
139 (3) recessive ($h=0$), where h is the dominance coefficient. To specify a set of simulation
140 parameters realistic for mammals, we chose parameters estimated in humans for

141 recombination rates and distribution of fitness effects. We use the UCSC exon map from the
142 HG19 genome and the Distribution of Fitness Effect (DFE) on non-synonymous mutations
143 estimated by (Eyre-Walker, Woolfit, & Phelps, 2006), assuming a non-synonymous mutation
144 rate of 7×10^{-9} per bp/generation and log additive interactions among selected loci. A summary
145 of the simulations is provided in Supplementary Table S1.

146 For all simulations, we have recorded fitness in the inbred population relative to that of
147 the outbred population, the ancestry proportion in the inbred recovering population, the
148 varying allele frequency of the adaptive mutation in the Mendelian model, and the fluctuation
149 of mean phenotype in the stabilizing selection model.

150

151 **3. Results**

152 *3.1 Selection on Mendelian traits*

153 We simulated a Mendelian trait that is fixed for the derived (locally adaptive) allele in the
154 recipient population, and fixed for the ancestral allele in the donor population. We varied the
155 selection coefficient on the trait, the dominance coefficient of the linked deleterious variation,
156 the admixture proportion during GR, and the demographic model (Model 1 vs. Model 2, see
157 Fig. 1).

158 We investigated the effect of GR on fitness in the recipient population (i.e. hybrid fitness,
159 Fig. 2 A-C) as well as on ancestral genome proportion (Fig. 2 D-F). Fitness is measured by
160 taking the average of the fitness of offspring in the recipient population, and normalizing by
161 the same quantity for the donor population. The fitness calculated in generation T is the
162 fitness of parents (rather than offspring produced) in generation T . We found that, depending
163 on the demographic model and dominance of deleterious variation, GR has drastically
164 different success in terms of achieving rapid increase in hybrid fitness. For example, when
165 deleterious mutations are partially recessive, GR is successful but somewhat slow for Model 2
166 (Fig. 2E). In Model 1, under the same scenario, fitness is not fully recovered even after 1000
167 generations post admixture with 10% admixture from the donor population (Fig 2B). By
168 contrast, under a fully recessive load, fitness is restored extremely quickly under Model 2,

169 provided sufficient admixture (1%), whereas with the same level of admixture in Model 1,
170 fitness is not restored even in the long run (>1000 generations post admixture) (Fig 2C).
171 Generally, we find that the lower the recipient fitness before admixture, the higher the amount
172 of genomic replacement by the donor population in the long run (Fig. 2D-F). Furthermore, the
173 more successful the GR is at restoring fitness, the higher the amount of genomic replacement
174 in the long run (Fig. 2C,F). These conclusions are similar to those previously observed by
175 Harris *et al.* (2019).

176 We also considered how ancestry and fitness evolve jointly in the recipient population
177 (Fig. 3). Here, we show dynamics for a population under Model 2 with recessive deleterious
178 variation. We found that in the first generation after GR, native ancestry is either 0 or 100% in
179 the parents, where native ancestry is associated with much lower fitness (Fig. 3A). After one
180 generation of admixture, a large proportion of offspring were inbred-outbred crosses, despite
181 low admixture proportion (1%). Due to the large fitness advantage associated with outbred
182 ancestry, these crossed individuals enjoyed much higher fitness than not only the inbred
183 individuals, but also the non-crossed outbred individuals, because it is extremely rare for
184 these crosses to be homozygous for recessive deleterious variation (it would require a
185 recessive deleterious variant to segregate in both inbred and outbred populations since
186 divergence up to the admixture). In the following generations, as ancestry proportions range
187 between ~30-90%, there is a clear trend of lower native ancestry incurring increased hybrid
188 fitness (Fig. 3C,D)

189 A short term bottleneck (Model 2) does not increase or decrease the average number of
190 mutations an individual carries. However, it will allow recessive deleterious mutations of
191 strong effect, which were already segregating in the population, to increase in frequency and
192 potentially go to fixation (while others are lost). Models of recessive mutations allow for
193 much more standing variation of deleterious mutations, that potentially can increase in
194 frequency during the bottleneck, than models of additive mutations (e.g. Fig. 2A vs 2C). GR
195 is particularly effective in this case because the recipient population may have fixed strongly
196 deleterious recessive mutations that can be purged immediately after GR (Fig. 2C). In the case

197 of a constant low population size (Model 1), deleterious mutations (both in the recessive and
198 additive model) will accumulate and can slowly go to fixation if they have weak effects, but
199 one is unlikely to observe the same kind of strong effect of strongly deleterious recessive
200 mutations going to fixation as you would in models with recessive mutations and a bottleneck
201 (Fig. 2B-C).

202 Next, we looked at the dynamics of local adaptations under a Mendelian trait model (i.e.,
203 a single adaptive allele). We found that, in the short term (0-100 generations post-GR) the
204 adaptive allele decreases in frequency following the loss of ancestral DNA fractions (Fig. 4;
205 Fig. S1), which is the consequence of a selection-induced reduction in native ancestry after
206 the admixture (Fig. 2D-F). However, while the ancestral genome proportion continued to
207 decline slowly after 10 generations after GR (Fig. 2D-F), the adaptive allele generally
208 increased in frequency after 10-100 generations when enough recombination occurred to
209 break up linkage between the adaptive allele and the deleterious alleles. However, even for
210 very strong selection ($s = 0.01$), it took hundreds of generations for the adaptive allele to reach
211 high frequency in the population. In some extreme cases, with sufficiently high levels of
212 admixture (10%), GR under Model 2 actually caused the adaptive allele to be lost with high
213 probability after a total genetic replacement when the selection coefficient is sufficiently small
214 (≤ 0.001) (Fig. 4F).

215 We also examined the joint effects of dominance coefficients of linked deleterious
216 variation and demographic history on the efficacy of GR. Under both model I and II, we saw a
217 greater degree of genetic replacement (Figure 2D-F), leading to a greater reduction in the
218 frequency of the adaptive allele, as deleterious mutations become more recessive (Fig. 3 &
219 S1). For example, there was a smaller short-term reduction in allele frequency of the adaptive
220 allele under Model 2 (Fig. 4D-F, Fig. S1 D-F, relative to Model 1 [Fig. 4A-C, Fig. S1 A-C])
221 but a larger reduction for partially recessive/recessive deleterious variants (Fig. 4B,C,E,F, Fig.
222 S1 B,C,E,F), following the same pattern of the ancestral DNA proportion decline in those
223 scenarios (Fig 4. G-H). However, the locally adaptive locus itself had only a minor effect on
224 the recovery of relative fitness and reduction of ancestral DNA proportion of the recipient

225 population (Fig. 4, 5, S1, S2, S3). We considered that sweeps from standing variation may
226 have different patterns of linked deleterious variation around the adaptive allele; however,
227 when simulating under alternative selection models we found no difference between the hard
228 vs soft sweep models (see Fig. 4, S2, S3 vs Fig. S4, S5, S6).

229

230 *3.2 Polygenic adaptation*

231 We also simulated a polygenic trait under a model of stabilizing selection with a shift in
232 the optimum (Fig. 5-7). Here we varied the strength of stabilizing selection on the trait
233 (controlled by $\sqrt{V_S}$, the ‘width’ of the fitness function), the size of the shift in the local
234 optimum after population 2 diverges from population 1, $\delta = 0,1,2,5$, measured in units of
235 $\sqrt{V_S}$), dominance coefficient of deleterious mutations, admixture fraction during GR as well
236 as demographic model.

237 We examined two features of polygenic trait evolution: first, we evaluated the effect of
238 GR on the perturbation of the adaptive phenotype from its optimum (Fig. 5, Fig. S7); we
239 measure this by looking at the average distance of the population mean phenotype from the
240 optimum. We also considered the extent of replacement of ancestral variation causal for the
241 trait (Fig. 6); we measure this replacement by examining the relative proportion of genetic
242 variance of the trait due to ancestral variation vs donor variation introduced by GR.

243 We found that under Model 1, polygenic adaptations are not significantly affected by GR,
244 as the trait’s evolution appears to follow the same trajectory regardless of admixture
245 proportions or dominance coefficients of the deleterious load (Fig. 5A-C). However, under
246 Model 2, we found that following rapid phenotypic drift from the optimum due to a severe
247 bottleneck (Fig. S7), polygenic adaptations subsequently follow dramatically different
248 trajectories depending on several factors (Fig. 5D-F): for example, GR allows the polygenic
249 adaptation to recover to its optimal value much more quickly than without GR (Fig. 5F); and
250 this effect is most pronounced under scenarios where there is fully recessive load (Fig. 5F),
251 although it is still significant under a partially recessive load (Fig. 5E).

252 We also explored how the genetic basis of the polygenic adaptation in the recipient

253 population is replaced by donor variation (Fig. 6). We quantify this using the proportion of the
254 genetic variance attributable to standing variation in the recipient population just before
255 admixture; genetic variance post-admixture is the sum of this quantity, plus genetic variance
256 attributable to standing variation in the donor population just before admixture, plus that of *de*
257 *novo* mutations occurring in the recipient population post-admixture (although this has
258 negligible contributions over short timescales). Generally, we find that the genetic basis is
259 quickly replaced due to GR, with >90% of the genetic variance being replaced with donor
260 variation when GR is most successful; for example, under Model 2, especially when the
261 deleterious load is recessive and the admixture fraction is high (Fig. 6A). Broadly, patterns of
262 genetic variance replacement are consistent with patterns of ancestry replacement (Fig. 6 *vs.*
263 Fig. 2D-F), with stronger replacement in situations where GR is more successful at recovering
264 fitness. However, details of the local adaptation do affect the dynamics of how the genetic
265 variance evolves; for example, when the optimal phenotype is more highly diverged in the
266 recipient *vs* donor population, the fraction of the genetic variance replaced by the donor
267 population is lower (Fig. 6B), because in this case donor individuals are more poorly adapted
268 to the environment of the recipient population, and thus GR is countervailed by this force.

269 Lastly, we directly compared hybrid fitness trajectories under the Mendelian *vs.*
270 polygenic trait models (Fig. 7). We found that, under the simulations models we considered,
271 varying parameters controlling the local adaptation does not have any appreciable effect on
272 hybrid fitness as an outcome of GR. In Fig. 7 we compare simulations of a Mendelian trait
273 under strong selection *vs.* a polygenic trait under strong stabilizing selection (see Methods).
274 The results are comparable both under Model 1 and Model 2 (Fig. 7A,B *vs* 7C,D) and under
275 various levels of dominance (Fig. 7).

276

277 **4. Discussion**

278 We have presented a population genetic simulation study that elucidates the dynamics of
279 local adaptation and genetic rescue (GR). We considered various models of the selection
280 strength and architecture of the adaptive trait, dominance of the mutational load, demography,

281 and admixture. The results of our simulations show that when a locally adaptive trait consists
282 of a single locus (e.g. a Mendelian trait), GR decreases the allele frequency in the short term.
283 Dominance of the linked deleterious variants and demographic history of the population
284 jointly determine the degree of its short-term loss while the strength of positive selection
285 determines the rate of trait recovery.

286 There are substantial differences in the evolutionary dynamics of the Mendelian trait and
287 the polygenic trait under GR. In simulations of a polygenic trait, the consequences of GR on
288 the trait is decided by both the loss of genetic materials as a whole and the distance between
289 the phenotype and its optimum before admixture. Generally speaking, it takes about 100
290 generations for a polygenic trait to return to its optimum in most cases, which is shorter than
291 that for a Mendelian trait under the same situation. Because polygenic traits have large
292 mutational targets, causal genetic variation that was previously exclusive to the donor
293 population is introduced to the inbred population via GR; this variation quickly replaces
294 native causal genetic variation, which is linked to many deleterious alleles. Thus, the
295 apparently higher efficiency with which the polygenic adaptation is restored comes at the cost
296 of long-term replacement by genetic variation from the donor population. We also showed
297 that the distance of the phenotypic optimum between the donor and the recipient population
298 has appreciable influence on how much genomic replacement is incurred by GR.

299 Our results demonstrate a marked difference between a long-term small effective
300 population size (Model 1) and a short-term severe bottlenecks (Model 2), with the latter
301 interacting strongly with the dominance of the deleterious mutation load. Our simulations
302 assume that, following GR/admixture, the effective population size of the recipient population
303 immediately recovers to the full size of the ancestral population. Future directions could
304 consider more gradual recoveries in the effective population size, possibly by using
305 evolutionary rescue models such as those discussed by Osmond & Coop (2019). Thus, our
306 models show GR operating at the upper limit of its efficiency, since the aforementioned
307 alternative models would have strictly lower effective population sizes in the short term
308 following admixture.

309 One caveat of our results is that our simulations do not assume epistasis and, therefore,
310 does not allow for the evolution of Dobzhansky-Muller incompatibilities (DMIs). However, in
311 the presence of DMIs, outbreeding depression may lead to limited genetic replacement or
312 even reduce the absolute fitness after GR.

313 Although our results suggest that locally adaptive traits, especially those that are
314 Mendelian or moderately polygenic, will be strongly affected by GR in the short term, but the
315 causal variant is generally retained and returns to fixation in the long run. While locally
316 adaptive polygenic traits are less susceptible to shifts due to GR, their underlying genetic
317 architecture is highly susceptible to long-term replacement by donor ancestry.

318

319 **References**

- 320 Adams, J. R., Vucetich, L. M., Hedrick, P. W., Peterson, R. O. & Vucetich, J. A. (2011).
321 Genomic sweep and potential genetic rescue during limiting environmental conditions in
322 an isolated wolf population. *Proc. R. Soc. B*.278:3336–3344.
- 323 Bell, D. A., Robinson, Z., Funk, W. C., Fitzpatrick, S. W., Allendorf, F. W., Tallmon, D. A., &
324 Whiteley, A. R. (2019). The Exciting Potential and Remaining Uncertainties of Genetic
325 Rescue. *Trends in Ecology and Evolution*, 34(12), 1070-1079.
- 326 Eyre-Walker, A., Woolfit, M., & Phelps, T. (2006). The distribution of fitness effects of new
327 deleterious amino acid mutations in humans. *Genetics*, 173(2), 891–900.
- 328 Fitzpatrick, S. W., Gerberich, J. C., Angeloni, L. M., Bailey, L. L., Broder, E. D., Torres-
329 Dowdall, J., Handelsman, C. A., López-Sepulcre, A., Reznick, D. N., Ghalambor, C. K.,
330 & Chris Funk, W. (2016). Gene flow from an adaptively divergent source causes rescue
331 through genetic and demographic factors in two wild populations of Trinidadian guppies.
332 *Evolutionary applications*, 9(7), 879–891.
- 333 Frankham, R., Ballou, J.D., Eldridge, M.D.B., Lacy, R.C., Ralls, K., Dudash, M.R. & Fenster,
334 C.B. (2011), Predicting the Probability of Outbreeding Depression. *Conservation*
335 *Biology*, 25: 465-475.
- 336 Frankham, R. (2015). Genetic rescue of small inbred populations: meta-analysis reveals large

- 337 and consistent benefits of gene flow. *Molecular Ecology*, 24(11), 2610-2618.
- 338 Frankham, R. (2016). Genetic rescue benefits persist to at least the F3 generation, based on a
339 meta-analysis. *Biol. Conserv.*, 195, 33-36
- 340 Haller, B. C., & Messer, P. W. (2019). SLiM 3: Forward Genetic Simulations Beyond the
341 Wright–Fisher Model. *Molecular Biology and Evolution*, 36(3), 632-637.
- 342 Harris, K., Zhang, Y., & Nielsen, R. (2019). Genetic rescue and the maintenance of native
343 ancestry. *Conservation Genetics*, 20(1), 59-64.
- 344 Hayward, L. K., & Sella, G. (2019). Polygenic adaptation after a sudden change in
345 environment. *bioRxiv*,
- 346 Heber, S., Varsani, A., Kuhn, S., Girg, A., Kempenaers, B., & Briskie, J. (2012). The genetic
347 rescue of two bottlenecked South Island robin populations using translocations of inbred
348 donors. *Proceedings. Biological sciences*, 280(1752), 20122228.
- 349 Hedrick, P. W., & Garcíadorado, A. (2016). Understanding Inbreeding Depression, Purging,
350 and Genetic Rescue. *Trends in Ecology and Evolution*, 31(12), 940-952.
- 351 Hedrick, P. W., Hellsten, U., & Grattapaglia, D. (2016). Examining the cause of high
352 inbreeding depression: analysis of whole - genome sequence data in 28 selfed progeny
353 of *Eucalyptus grandis*. *New Phytologist*, 209(2), 600-611.
- 354 Hedrick, P. W., Robinson, J. A., Peterson, R. O. & Vucetich, J. A. (2019) Genetics and
355 extinction and the example of Isle Royale wolves. *Anim. Conserv.*, 22(3), 302-309
- 356 Hwang, A. S., Northrup, S. L., Peterson, D. L., Kim, Y., & Edmands, S. (2012). Long-term
357 experimental hybrid swarms between nearly incompatible *Tigriopus californicus*
358 populations: persistent fitness problems and assimilation by the superior population.
359 *Conservation Genetics*, 13(2), 567-579.
- 360 Johnson, W. E., Onorato, D. P., Roelke, M. E., Land, E. D., Cunningham, M. W., Belden, R.
361 C., ... & Obrien, S. J. (2010). Genetic Restoration of the Florida Panther. *Science*,
362 329(5999), 1641-1645.
- 363 Kyriazis, C. C., Wayne, R. K., & Lohmueller, K. E. (2019). High genetic diversity can
364 contribute to extinction in small populations. *bioRxiv*.

- 365 Madsen, T., Shine, R., Olsson, M. et al. (1999). Restoration of an inbred adder population.
366 Nature 402, 34–35.
- 367 Osmond, M. M., & Coop, G. (2019). Genetic signatures of evolutionary rescue by a selective
368 sweep. bioRxiv.
- 369 Prufer, K., Racimo, F., Patterson, N., Jay, F., Sankararaman, S., Sawyer, S., ... & Paabo, S.
370 (2014). The complete genome sequence of a Neanderthal from the Altai Mountains.
371 Nature, 505(7481), 43-49.
- 372 Simons, Y. B., Bullaughey, K., Hudson, R. R., & Sella, G. (2018). A population genetic
373 interpretation of GWAS findings for human quantitative traits. *PLoS biology*, 16(3),
374 e2002985.
- 375 Smyser, T. J., Johnson, S. A., Page, L. K., Hudson, C. M., & Rhodes, E. J. (2013). Use of
376 experimental translocations of Allegheny woodrat to decipher causal agents of decline..
377 Conservation Biology, 27(4), 752-762.
- 378 Tallmon, D. A., Luikart, G., & Waples, R. S. (2004). The alluring simplicity and complex
379 reality of genetic rescue. *Trends in Ecology and Evolution*, 19(9), 489-496.
- 380 Tomasini, M., & Peischl, S. (2019). When does gene flow facilitate evolutionary rescue.
381 bioRxiv.
- 382 Whiteley, A. R., Fitzpatrick, S. W., Funk, W. C. & Tallmon, D. A. (2015) Genetic rescue to
383 the rescue. *Trends in Ecology & Evolution* 30: 42-49.

384

385 **Data accessibility**

386

387 Scripts are available on GitHub at https://github.com/YulinZhang9806/GR_adaptation_scripts.

388

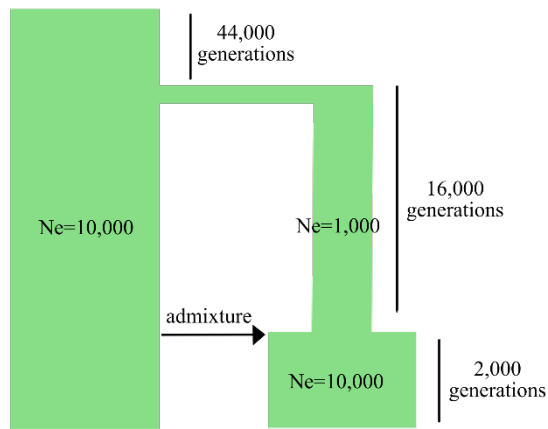
389 **Authors contribution**

390

391 AJS and RN conceptualized the study; YZ and AJS designed the methods; YZ wrote the
392 software; YZ and AJS conducted the analysis; YZ and AJS wrote the manuscript; YZ, AJS, and
393 RN edited the manuscript; AJS and RN supervised the research.

394

A. Model 1



B. Model 2

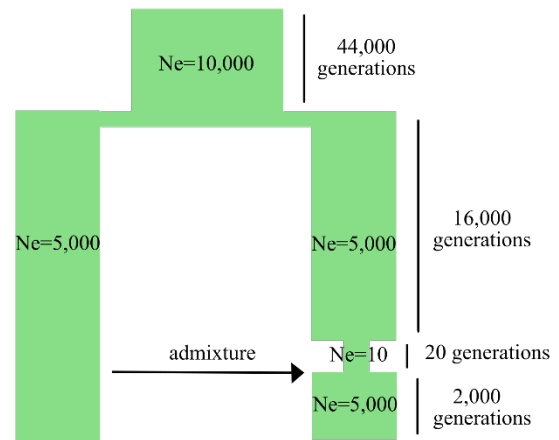


Figure 1. Two demographic models used for simulations. Time runs from top to bottom. Admixture happens at the generation right after the population size increases and lasts for only one generation. Population size changes are assumed to be discrete as depicted in the figure. Samples are taken from the inbred population on the right (p_2) after the admixture up to 2,000 generations.

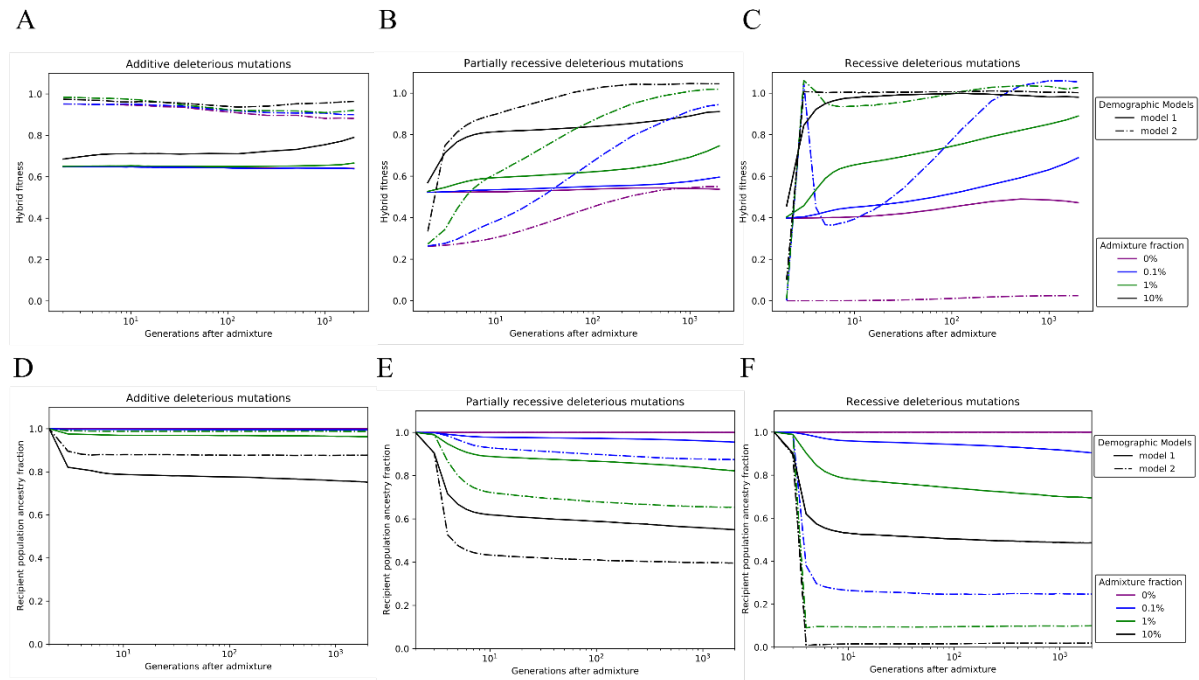


Figure 2. (A-C) Hybrid fitness change of the inbred population after admixture and (D-F) Recipient population ancestral genome fraction changes after GR with a Mendelian adaptive trait, under hard sweep selection model and demographic Model 1 (solid lines) and demographic Model 2 (dashed lines). The adaptive mutation is additive (dominance coefficient $h=0.5$) while selection coefficient is set differently (shown with different line styles in A-F). Deleterious mutations are assumed additive ($h=0.5$) in A, D, partially recessive ($h=0.1$) in B,E and recessive ($h=0$) in C,F.

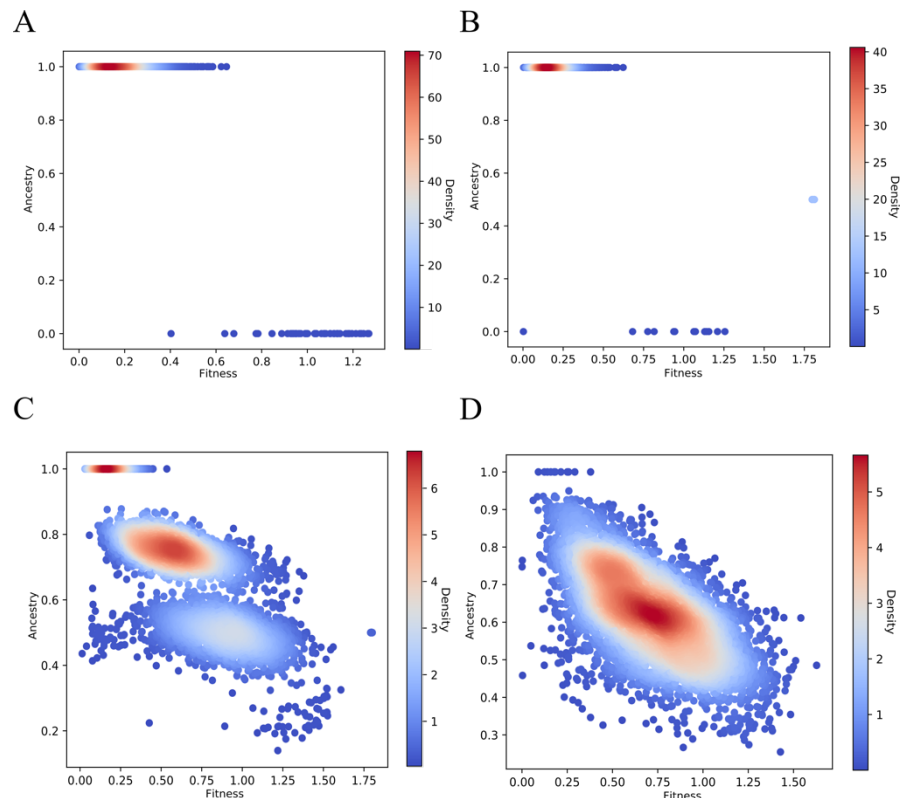


Figure 3. Relation between individual fitness and its ancestral genome proportion under demographic Model 2, with recessive deleterious mutations and admixture fraction of 1%. Each dot represents an individual, depicting relation between ancestry proportion and relative fitness (to the mean fitness of the outbred population) of each individual in the inbred recipient population. Figure A shows the population before mating with outbred individuals. Figure B indicates the first generation after admixture (e.g. F1), while figure C represents the second generation (e.g. F2) and figure D shows the third generation (e.g. F3).

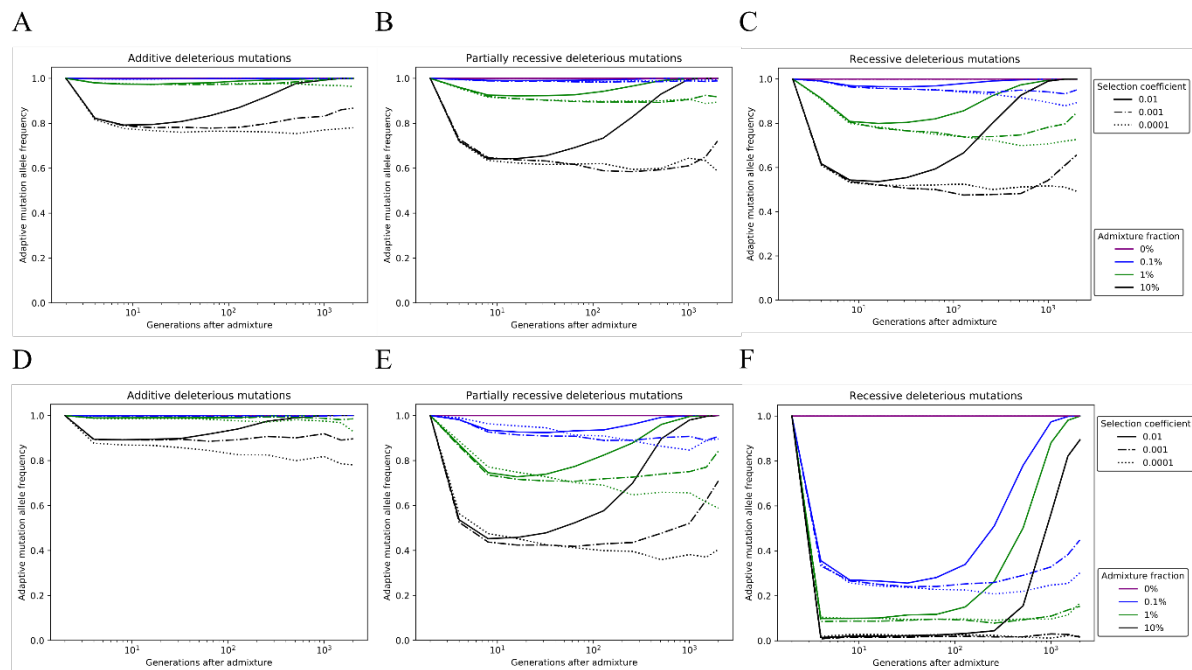


Figure 4. Allele frequency changes after admixture for a Mendelian trait under hard sweep selection model and (A-C) demographic Model 1 (D-F) demographic Model 2. The adaptive mutation is additive (dominance coefficient $h=0.5$) while selection coefficient is set differently (shown with different line styles). Deleterious mutations are assumed additive ($h=0.5$) in A, D, partially recessive ($h=0.1$) in figure B,E and recessive ($h=0$) in C,F.

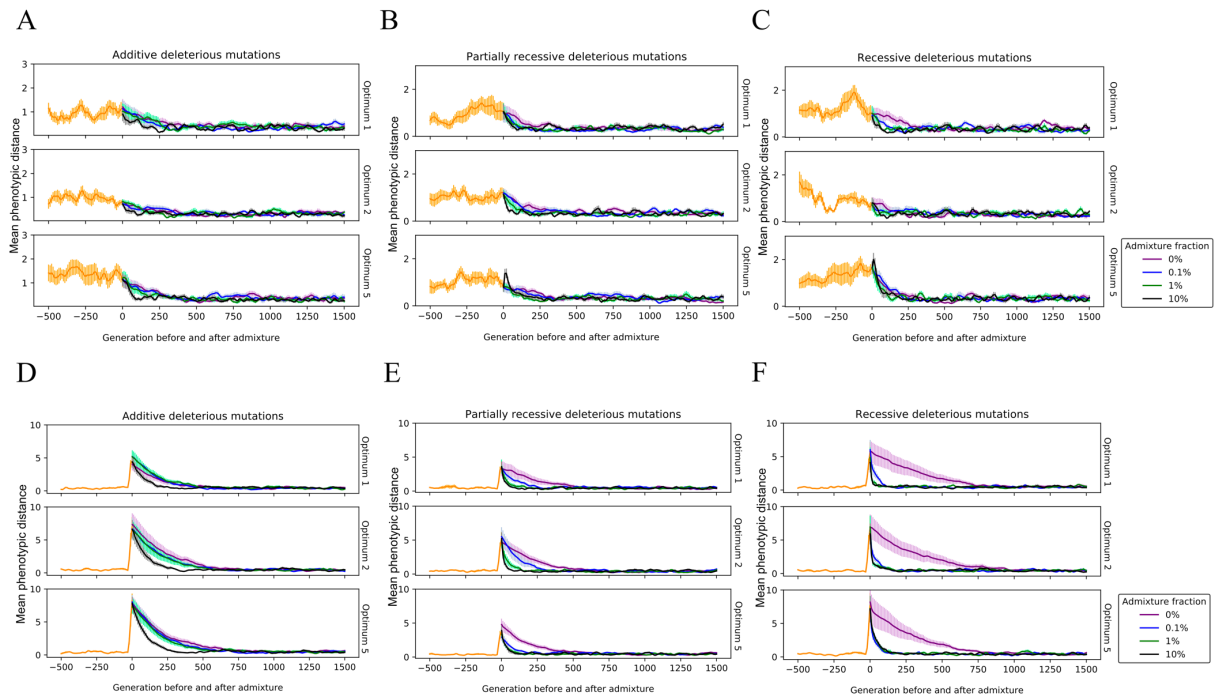


Figure 5. Mean phenotype distance from optimum over time. (A-C) Simulations under Model 1, (D-F) simulations under Model 2. Shaded bars signify 95% confidence intervals for the mean phenotypic distance.

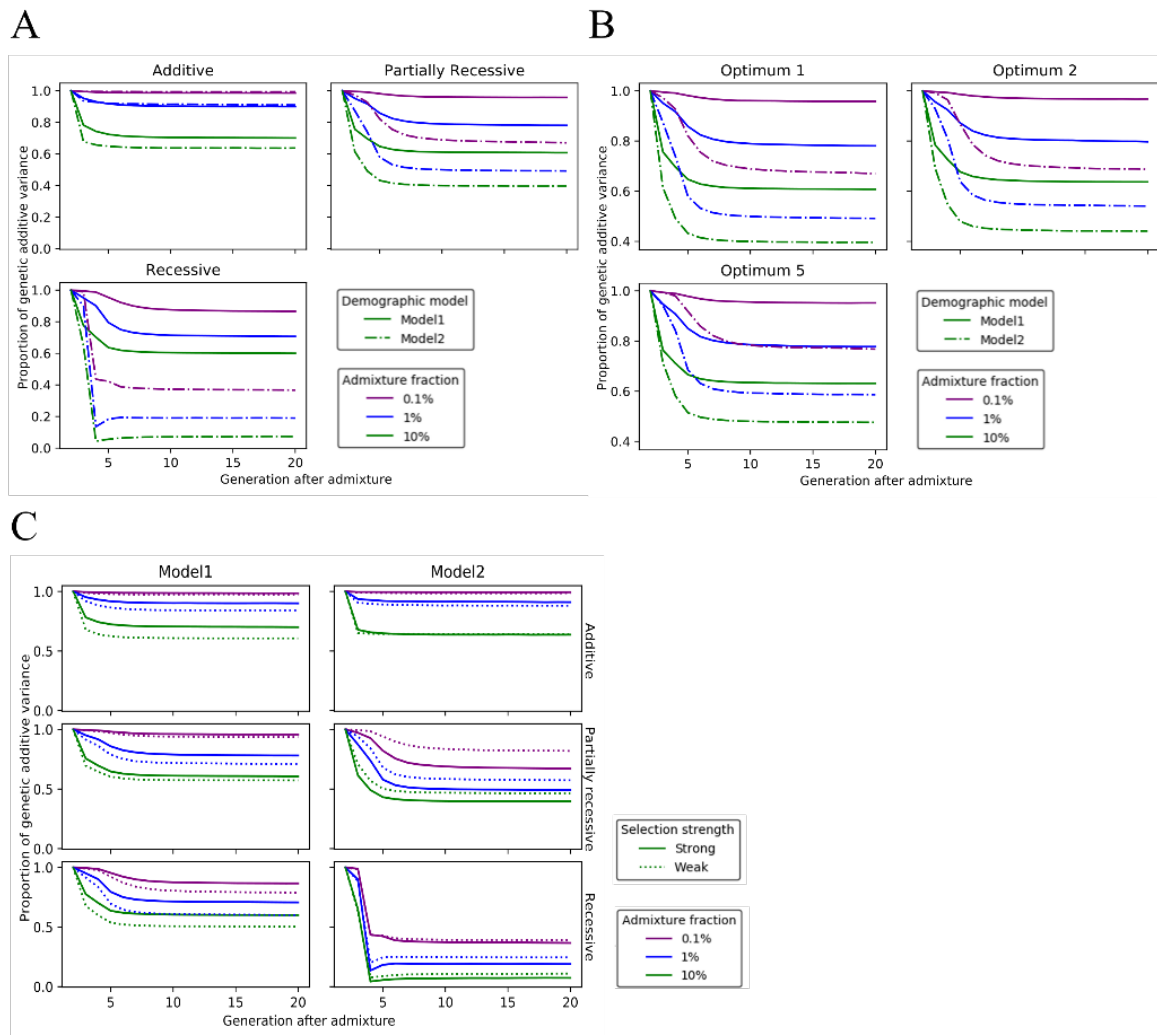


Figure 6. Proportion of genetic additive variance of a polygenic adaptation, recording mutations that originate from the recipient population for 20 generations after GR. (A) Scenarios under strong selection, with optimum of 1 for the recipient population and different dominance coefficients for deleterious mutations. (B) Scenarios under strong selection, with partially recessive deleterious mutations and different optimum for the recipient population. (C) Scenarios with optimum equals 1 and different selection strength for the adaptive trait. Each line represents the proportion of genetic additive variance contributed by variants, which compose the trait, from the ancestral genome of inbred population. Here, genetic additive variance is calculated as $G = \sum_{l \in SNPs} 2a_l^2 p_l (1 - p_l)$, where a_l represents the effect of SNP l , and p_l its frequency.

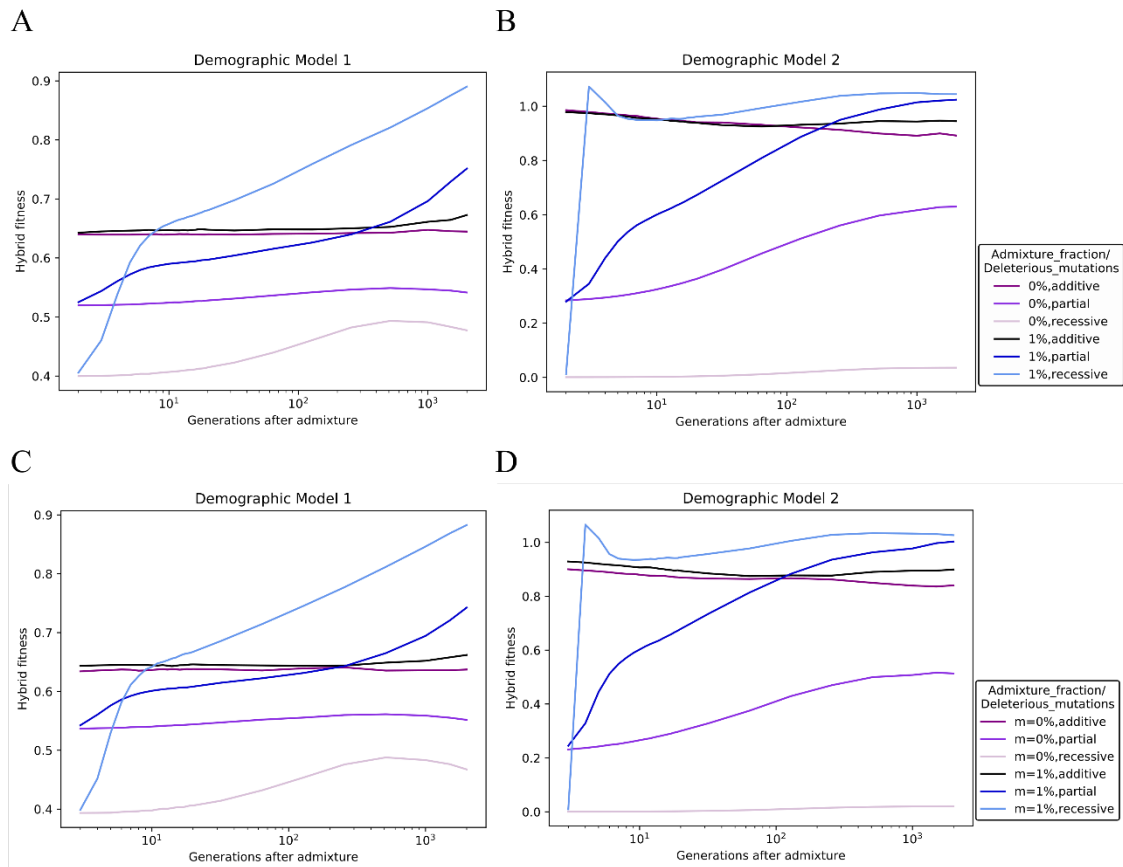


Figure 7. Hybrid fitness changes of the inbred population after admixture with (A-B) a Mendelian adaptive trait, under hard sweep selection model and (C-D) a polygenic trait under stabilizing selection with strong selection. Figure A and C are results of demographic Model 1 while B and D are that of demographic Model 2. Lines of different colors are indicating scenarios with different admixture fraction and dominance (of deleterious mutations).